

# The Film Formation of Acrylic Latexes: A Comprehensive Model of Film Coalescence

SARAH T. ECKERSLEY<sup>1</sup> and ALFRED RUDIN<sup>2,\*</sup>

<sup>1</sup>Dow Chemical, 1604 Building, Midland, Michigan 48674; <sup>2</sup>Department of Chemistry, Institute for Polymer Research, University of Waterloo, Waterloo, Ontario, Canada

## SYNOPSIS

A comprehensive model of film formation that was proposed in an earlier article by the present authors was evaluated for latexes having a wide range of physical properties. In this model, capillary force and interfacial forces act in tandem to promote film coalescence. The emulsion polymers studied were all based on poly(methyl methacrylate-co-butyl acrylate). The viscoelastic nature of the copolymer was varied by the addition of molecular weight modifiers (CBr<sub>4</sub> chain-transfer agent and ethylene glycol dimethacrylate cross-linking monomer) during synthesis. In contrast to the simplifications of the previous analysis, the experimental system was well characterized. The effect of water plasticization was investigated. The surface energetics of the system were studied. Also, drying kinetics were considered. Results showed that the degree of coalescence ranged from complete fusion to superficial fusion. The minimum film temperature was found to increase with increasing polymer rigidity, as is expected. Comparison of the model predictions and experimental observations validated the model. © 1994 John Wiley & Sons, Inc.

## INTRODUCTION

Water-based coatings are becoming increasingly important as the range of applications of these materials widens. Currently, worldwide efforts are aimed at reducing the volatile organic solvent content of most coating materials, particularly those employed in automotive manufacture. This has promoted the search for a new generation of high-performance water-based coatings to replace the older solvent-based technology. An understanding of the scientific principles governing the properties of the former materials is essential to further innovation.

Water-based coatings comprise of an array of chemical components. These range from inorganic opacifying pigments such as titanium dioxide to organic surface active agents and plasticizers. The primary ingredient is the polymeric binder latex. The binder film provides a vehicle for secondary ingredients, mechanical integrity, and protection of the substrate. The process of film formation from latex

coatings influences the final film performance, since the quality of the film formed dictates the ultimate properties of the coating. Hence, study of the film-formation process is of paramount importance in understanding water-borne coating behavior.

As a film-forming latex dries, it is transformed from a dispersion of polymer particles in a continuous water phase to a dry polymer film. The drying of latex films is considered to occur in three stages: A constant drying rate is maintained during the first stage as bulk water evaporation takes place. In the second stage, when sufficient water has evaporated to bring the polymer particles into irreversible contact, the evaporation rate begins to fall and the film fusion process is initiated. The second stage of drying is complete when virtually all the water has evaporated and a nascent film has formed. Finally, in the third stage, residual water diffuses from the film. The dry film undergoes "further gradual coalescence,"<sup>1</sup> becoming increasingly homogeneous upon aging. The process, termed autohesion,<sup>2</sup> is the diffusion of polymer chain ends across the inter-particle boundaries.

Several mechanistic models of film formation have been developed in the past. A dry sintering

\* To whom correspondence should be addressed.

model was proposed by Bradford et al.,<sup>3</sup> where fusion of the dry latex is caused by the tendency to reduce surface energy. The driving force is the polymer surface tension. In subsequent models, film coalescence is promoted either by the surface tension of water in the channels between particles<sup>4-8</sup> or the polymer/water interfacial tension.<sup>9</sup> In a previous article<sup>10</sup> by the present authors, these models were evaluated. It was found that they did not fully account for experimental observations. Hence, a comprehensive model of film formation was proposed, in which the capillary and interfacial forces are complementary.

The radius of the contact region " $a$ " between the particles is the sum of the contributions from the capillary and interfacial forces. The capillary force component results from the presence of water capillaries in the interstitial regions between the particles. The interfacial force component arises from the tendency of spheres in contact to reduce surface area. The deformations due to each force component are additive, provided the material behaves in a linear viscoelastic manner. The radius of the circle of contact is given by the general expression

$$a = a_{\text{capillary}} + a_{\text{interfacial}} \quad (1)$$

The model predicts the radius of the circle of contact ( $a$ ) between monodisperse coalesced latex particles as a function of the following latex properties: latex particle radius ( $R$ ), elapsed drying time ( $t$ ), polymer modulus ( $G^*$ ),<sup>†</sup> and polymer viscosity ( $\eta^*$ ),<sup>‡</sup> according to eq. (2):

$$a = \left( \frac{2.80R^2\sigma}{G^*} \right)^{1/3} + \left( \frac{3\gamma Rt}{2\pi\eta^*} \right)^{1/2} \quad (2)$$

The driving force for the process is the tendency to reduce surface energy, both in the water capillaries (or channels) between adjacent particles and between the contacting latex particles. The magnitude of the driving force promoting fusion is governed by the surface tension of water in the interstitial capillaries ( $\sigma$ ) and the polymer/water interfacial tension ( $\gamma$ ). The reader is referred to the original article for the mathematical derivations.<sup>10</sup>

The model was evaluated experimentally in the previous study<sup>10</sup> by varying the particle radii of latexes having identical chemical compositions (and, consequently, single values of the other parameters

at a given temperature). It was shown that the predicted and experimental values of the radius of the circle of contact " $a$ " were in agreement.

Several approximations were allowed in the former analysis. In the current analysis, the comprehensive model is subject to further examination using experimentally determined values of the thermodynamic and viscoelastic parameters rather than estimates.

These refinements are detailed below. In the first study, the surface energies of the latex system were estimated. In subsequent work,<sup>11</sup> these quantities were determined experimentally. In addition, a measured value of the water capillary surface tension is employed here.

The models of film formation by coalescence of latex particles that have been cited above involve different driving forces. These are dry sintering (air/polymer interfacial tension), water/air surface tension, polymer/water interfacial tension, or a combination of the latter two factors. Except for the dry sintering model, all theories assume a connection between drying and coalescence. Our study<sup>12</sup> of the drying of polymer particles with different morphologies is consistent with a model<sup>13</sup> in which evaporation occurs from a water surface that retreats through the film as drying proceeds. The upper layer of the film is dry and porous and the water in the lower, wet layer supplies moisture to maintain a constant evaporation rate.

This percolation model implies that drying is complete prior to coalescence. This conclusion affects the analysis of the film-formation process, since both wet and dry sintering must be occurring. The presence of water (or its absence) in the film during the coalescence process determines the various interfacial energies and affects the viscoelastic properties of the polymer.

Evidently, water is an indispensable ingredient in emulsion polymerizations. It is conceivable that water could have a plasticizing effect on film-forming copolymers, particularly those possessing some hydrophilic character. Since water is present in varying concentrations throughout the film-formation process, it is important to determine the influence of water on the film-fusion process. Dynamic mechanical measurements were employed in a previous study<sup>14</sup> to investigate water plasticization of a series of poly (butyl acrylate-*co*-methyl methacrylate) latexes having varying polymer morphologies. These same materials are employed in the current study. The results indicated that significant water plasticization occurred when the materials were exposed to water for extended periods of time.

<sup>†</sup> The complex modulus,  $G^*$ , of a material is  $G^*(\omega) = G'(\omega) + iG''(\omega)$ , where  $G'$  is the storage modulus and  $G''$  is the loss modulus.

<sup>‡</sup> The complex viscosity  $\eta^* = G^*(\omega)/i\omega$ , where  $\omega$  is the test frequency.

All the above-mentioned refinements are incorporated into the current assessment of the model. However, the main focus of the present research is to evaluate the model using more exacting criteria than those of Ref. 10. To this end, a series of mono-disperse film-forming latexes were prepared that differed in physical properties while retaining virtually identical chemical compositions. This was accomplished via the addition of molecular weight modifiers  $\text{CBr}_4$  (carbon tetrabromide) and  $\text{Cl}_4$  (carbon tetraiodide) chain-transfer agents and ethylene glycol dimethacrylate (EGDM, cross-linking agent) to the emulsion polymerization. At room temperature, the moduli of these materials range over nearly two orders of magnitude. Therefore, these latexes represent a critical test of the validity of the comprehensive model of film formation.

The minimum film temperature (MFT) is of less consequence scientifically than is the mechanism of film fusion. However, it is of great commercial import. Earlier work<sup>10,15</sup> indicated that the MFT monotonically increased with increasing particle size. Simple reasoning predicts that as the cross-link density of the polymer is increased the MFT should increase since the flow and deformation of the material are restricted.

## EXPERIMENTAL

### Emulsion Polymerization

Latexes were synthesized using a semicontinuous reaction scheme. The proportions of all reactants, except for the molecular weight modifiers, were kept constant between the various recipes. The basic emulsion polymerization recipe is given in Table I. Table II provides information about the molecular weight modifiers used and the resulting particle size and particle-size distributions. Two seeded reactions were performed (L2 and L11). In both cases, the second-stage concentrations were all identical to the seed concentrations.

**Table I** Surfactant Free-emulsion Polymerization

Reactor charge	
Deionized water	210 g
Ammonium persulfate initiator	1.35 g
Monomer mixture	
Butyl acrylate	101.4 g
Methyl methacrylate	101.4 g
Methacrylic acid	2.55 g
Molecular weight modifier	$x$ g

**Table II** Emulsion Polymer Molecular Weight Modifiers and Particle-size Distributions

Latex	Modifier	$x$ (g) <sup>b</sup>	$D_n$ (nm)	$D_w/D_n$
L1 <sup>a</sup>	$\text{CBr}_4$	5.00	671	1.010
L2	$\text{CBr}_4$	5.00	890	1.010
L3	$\text{CBr}_4$	2.50	680	1.030
L4	$\text{CBr}_4$	0.96	606	1.010
L5	$\text{Cl}_4$	0.10	647	1.005
L6	—	—	580	1.010
L7	EGDM <sup>c</sup>	0.40	582	1.020
L8	EGDM <sup>c</sup>	0.50	588	1.010
L9	EGDM <sup>c</sup>	1.50	438	1.020
L10 <sup>d</sup>	EGDM <sup>c</sup>	3.00	699	1.010
L11	EGDM <sup>c</sup>	3.00	1002	1.010
L12	EGDM <sup>c</sup>	8.00	899	1.007
L13	EGDM <sup>c</sup>	12.00	984	1.006

<sup>a</sup> Seed for L2.

<sup>b</sup> Refer to recipe in Table I.

<sup>c</sup> Ethylene glycol dimethacrylate.

<sup>d</sup> Seed for L11.

All reactions were carried out in a 1 L kettle reactor equipped with an overhead condenser and a jacketed mechanical stirrer. The stirring rate was maintained at 250 rpm throughout the reaction.

The water and initiator were charged to the reactor and maintained at a temperature of 80°C with continuous stirring. The monomer mixture was fed to the reactor via a fluid metering pump at a constant rate of approximately 1 mL min<sup>-1</sup>. No monomer accumulation was observed at any time. Therefore, it was assumed that the reaction was starve-fed and that the composition of the terpolymer was uniform throughout the latex particle. When monomer addition was complete, the reaction was continued for 1 h. The latex was then gradually cooled to ambient temperature. Finally, the latex was filtered through a 100-mesh screen to remove the minimal amount of grit formed during the polymerization. Latex particle-size measurements were obtained using an ICI-Joyce Loeb Disk Centrifuge according to a method described elsewhere.<sup>16</sup> Molecular weight measurement was prohibited because most of the copolymers were cross-linked to some extent. The estimation of gel content by Soxhlet extraction was attempted, but the reproducibility was poor.

### Water-phase Surface Tension

The latexes synthesized for this study are subject to settling under the influence of gravity. It was desired to separate the continuous phase from the polymeric phase. Hence, the latex was allowed to

separate and the liquid phase was decanted. The liquid was centrifuged at 2700 rpm for a period of approximately 2 h. The supernatant liquid was decanted, and the procedure was repeated.

The liquid surface tensions were measured using a calibrated ring tensiometer. Five replicate measurements were made for each of the four latexes. The values of the surface tension averages, along with 95% confidence intervals, are given in Table III. Evidently, there is an effect of the polymerization recipe on the surface tension of the supernatant liquid. This is likely due to the presence of impurities and oligomeric surface active molecules (generated from the initiator and monomer) in the continuous phase. However, because of the relatively small differences between samples, the values of the surface tensions were averaged, and the mean was used as an adequate approximation of the continuous phase surface tension ( $\sigma$ ).

### Scanning Electron Microscopy (SEM) and Minimum Film Temperature (MFT)

An apparatus similar to that used by Protzman and Brown<sup>17</sup> and ASTM method D2354 (Ref. 18) was used to determine the MFT of the various latexes. An insulated stainless-steel bar replaces an aluminum bar in the original apparatus. Cooling at one end of the bar is achieved by two 12-V ceramic thermoelectric cooling modules. The cooling rate was maintained by means of a feedback control device. Heat was not applied at the opposite end of the bar, since all the MFTs were below room temperature. The temperature gradient along the bar was determined by eight thermocouples installed at intervals along the bar. The thermocouples were connected to a digital temperature indicator that had an accuracy of  $\pm 0.1^\circ\text{C}$ .

A glass plate that permitted visual observation of the drying films covered the stainless-steel bar. Prior to application of the latexes, the cooling mechanism

was activated and nitrogen gas flow from the cold to hot end of the bar at a rate of 2000 mL/min was started. The nitrogen gas minimized condensation of water at the cold end of the bar and maintained the humidity at a constant level. The temperature of the bar was allowed to equilibrate for about 6 h. The glass plate was removed, approximately equal volumes of the latexes were applied to the channels down the length of the bar, and the glass plate was quickly replaced. Drying of the latexes took approximately 4 h. During this time, five replicate measurements of the temperature gradient along the bar were obtained and subsequently averaged. The MFT was determined as the temperature at which clarity of the dry film was observed.

The coalescence behavior of the dried latex cast films was examined by SEM. Prior to exposure to the electron beam, the films were gold-sputtered to a thickness of  $1.6 (10^{-4})$  m to prevent charging and deformation of the film surface.

## RESULTS AND DISCUSSION

### MFT and SEM

Past work focused on the effect of particle size on MFT. In the present study, the effect of polymer structure is investigated. Table IV lists the MFTs for the full range of latexes considered. It is evident that the addition of molecular weight modifiers has a pronounced effect on the MFT. As the level of the chain-transfer agent is increased, the MFT decreases. The effect of particle size on MFT was demonstrated in an earlier article and is reinforced by the results for two-stage syntheses (L1/L2 and L10/L11). A statistical analysis of the MFT results was not done, primarily because there are insufficient data to perform a multivariate analysis.

Scanning electron micrographs of latex films dried at room temperature ( $T = 22^\circ\text{C}$ ) are depicted in Figure 1. The micrographs parallel the MFT data and show the expected behavior. The trend agrees with the emulsifier exudation studies of Bradford and Vanderhoff<sup>19</sup> on styrene/butadiene copolymers modified with divinylbenzene and *t*-dodecyl mercaptan.

These observations and the MFT results are as expected since the addition of molecular weight modifiers influences the mobility of the polymer. The cross linker restricts the motion of the matrix and, in the extreme case, prohibits permanent deformation. The chain-transfer agent not only reduces the molecular weight, but it also increases the chain-end concentration, thus promoting interpenetration

**Table III** Surface Tensions of Latex Continuous Phases

Latex	Surface Tension, $\sigma$ (mJ m <sup>-2</sup> )	95% Confidence Interval for $\sigma$
L1	50.34	0.24
L6	49.78	0.14
L12	48.92	0.27
L13	46.28	0.16
Average	48.83	0.75

**Table IV** Minimum Film Temperature (MFTs) of Modified Latexes

Latex	Modifier	Weight % Modifier <sup>a</sup>	MFT (°C)	95% Confidence Interval for MFT (°C)
L1 <sup>b</sup>	CBr <sub>4</sub>	1.172	8.0	0.5
L2	CBr <sub>4</sub>	1.172	12.0	1.8
L3	CBr <sub>4</sub>	0.600	9.9	0.1
L4	CBr <sub>4</sub>	0.227	11.5	0.4
L5	Cl <sub>4</sub>	0.024	11.9	0.9
L6	—	—	11.0	0.3
L7	EGDM	0.097	12.6	0.9
L8	EGDM	0.118	12.7	1.0
L9	EGDM	0.371	14.0	0.5
L10 <sup>c</sup>	EGDM	0.720	14.0	0.9
L11	EGDM	0.720	15.8	1.5
L12	EGDM	1.890	18.6	1.6
L13	EGDM	2.741	21.4	1.6

<sup>a</sup> Based on total emulsion mass.

<sup>b</sup> Seed for L2.

<sup>c</sup> Seed for L11.

across the particle boundaries. The results of both techniques suggest that a high concentration of the chain-transfer agent in the emulsion polymerization is advantageous. When cast, the latex produces a homogeneous, fully fused film having a low MFT. This notion must be tempered by the realization that an excess of the chain-transfer agent will yield a weak film. Also, at concentrations of CBr<sub>4</sub> and Cl<sub>4</sub> comparable to that of latexes L1, L2, L3, and L5, noticeable discoloration of the dry film becomes apparent. Therefore, it appears that an intermediate level of a molecular weight modifier generates the optimum film.

A cautionary comment about MFT measurements: For the very cross-linked systems (such as L12 and L13), visual inspection suggests that a hazy film has formed at  $T > \text{MFT}$ . Examination of the corresponding electron micrographs shows a deformed but barely coalesced film that is subject to water whitening. It can be postulated that the interstitial voids are rendered sufficiently small by the deformation that visible light is not scattered by the particles, giving the illusion of a homogeneous surface.

## Comprehensive Model of Film Formation

### Data Analysis

As discussed in the Introduction, the parameters that had been previously estimated in the prelimi-

nary evaluation of the model<sup>10</sup> were actually measured in succeeding research. However, because of the nature of the measurements, minor approximations are still required. As noted in the Experimental section, the surface tension of the continuous water phase was approximated by a single value rather than by individual values corresponding to individual polymerizations.

The model will be assessed by comparison of experimental and predicted values of “ $a$ ” from eq. (2) at the drying temperature of the films ( $T = 22^\circ\text{C}$ ). Thus, values of the viscoelastic parameters are required at this specific temperature. Interpolation of  $\log G^*$  (or equivalently,  $\log \eta^*$ ) data as a function of temperature data was necessary. This was accomplished by generating an empirical polynomial expression (in the immediate region of  $22^\circ\text{C}$ ) for  $\log G^*$  as a function of temperature and then interpolating.

The dynamic mechanical experiments of Ref. 14 demonstrated that the polymer underwent water imbibition, causing a reduction in the modulus. It is assumed that water plasticization has an effect on film formation. Reasonable values of the reduced modulus (and viscosity) are required for calculations. The experimental rheological measurements during temperature sweeps of the water-treated polymers do not furnish exact measurements. This is an unavoidable consequence of the method of data acquisition. The viscoelastic properties of the polymers vary widely; therefore, each polymer must be treated uniquely. For instance, the most cross-linked materials are exposed to elevated temperatures to ensure adhesion to the rheometer plates. This is prohibited with the low molecular weight specimens. Consequently, an unknown quantity of water evaporates during sample loading. Nevertheless, inspection of the room temperature ( $22^\circ\text{C}$ ) data revealed that the ratio of  $\log G^*$  of the dry polymer to  $\log G^*$  of the water-exposed sample was very close for all the polymers studied. It was decided to calculate a single value for the ratio  $\log G^*(\text{wet}) : \log G^*(\text{dry})$  from an average of all the individual values. The relationship found was  $\log G^*(\text{wet}) = 0.90 \log G^*(\text{dry})$ , or  $G_{\text{wet}}^* = G_{\text{dry}}^{*0.90}$ . Since the individual values are not completely reliable, this approach was deemed the most sensible.

### Model Evaluation

The mechanism of latex film drying implicitly affects the analysis of the film-fusion process. Two mechanistic models<sup>13,20</sup> of latex-drying kinetics were reviewed in Ref. 12. It was demonstrated that Croll's<sup>13</sup>

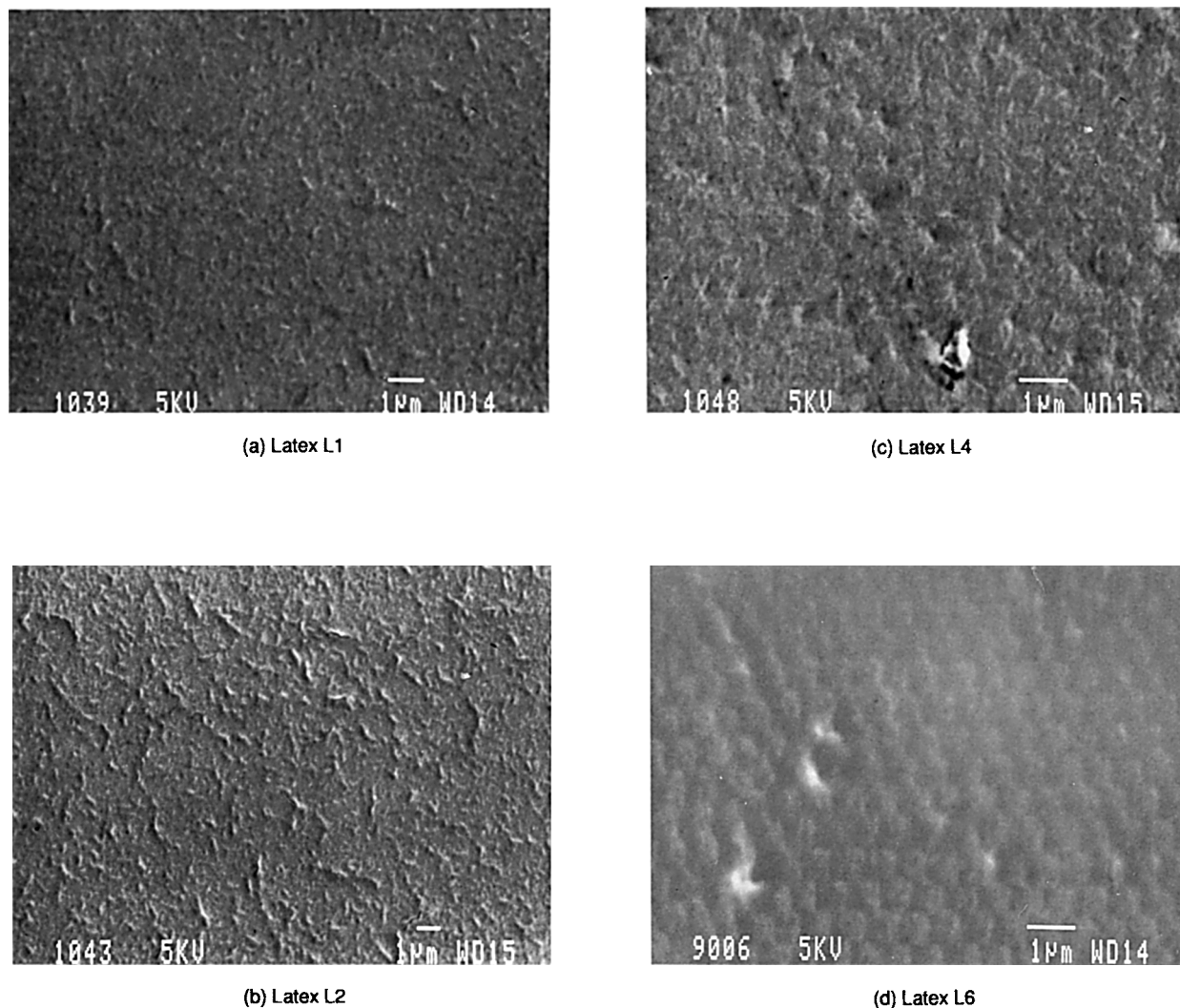


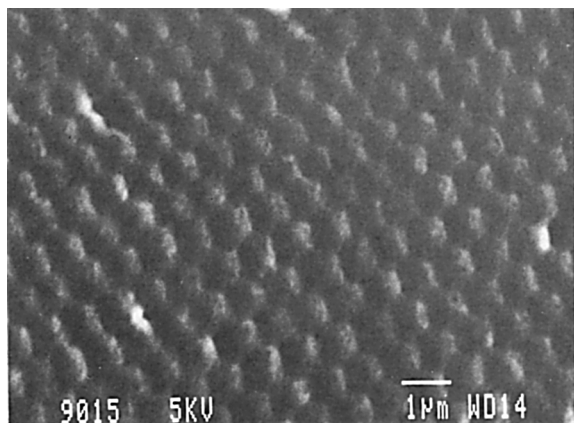
**Figure 1** Scanning electron micrographs of latex films synthesized with molecular weight modifiers.

model best fit the experimental data. In the first stage of this model, a drying front passes through the film toward the substrate, leaving behind a dry porous layer. In the second stage, the rate falls as the drying front approaches the substrate.

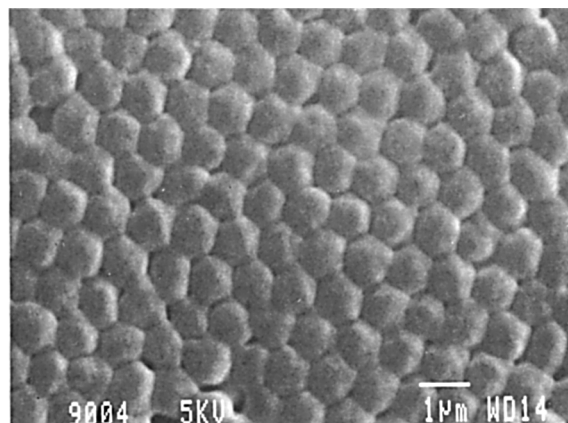
The duration of the first stage depends on the initial mass of latex. However, the elapsed time between the beginning of stage 2 and the time the rate begins to plateau toward zero is consistently close to 2 h. It was assumed that the capillary force acts on the particles as the drying front passes. Contact is then established, and deformation continues under the influence of interfacial tension.

Croll's model suggests that the coalescence of stage 2 should be controlled by the polymer/air interfacial tension, since the porous outer layer is os-

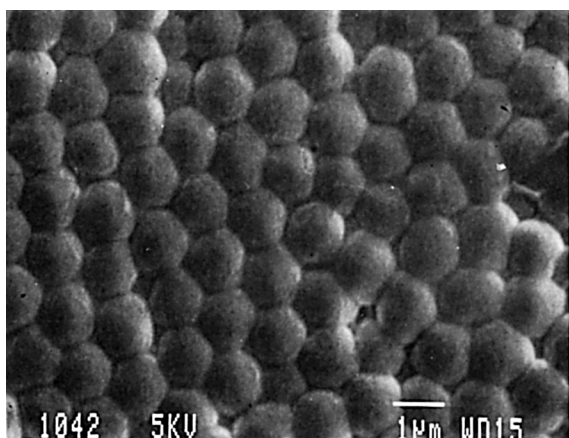
tensibly dry. It is debatable whether the polymer is truly dry (since there is a constant flux of water vapor through the channels of the porous region) or whether it retains absorbed water. Consequently, the model of film formation can be evaluated under two extreme conditions: The material can be considered to be fully dry at the start of the falling rate period, in which case the dry viscoelastic parameters will apply. The driving force during the second stage will then be the polymer/air interfacial tension ( $\gamma_{p/a}$ ). If, alternatively, the polymer retains a significant quantity of water, the wet viscoelastic parameters and the polymer/water interfacial tension ( $\gamma_{p/w}$ ) will apply. It is not feasible to determine the precise conditions of the film throughout the drying period. Therefore, it was decided to evaluate the



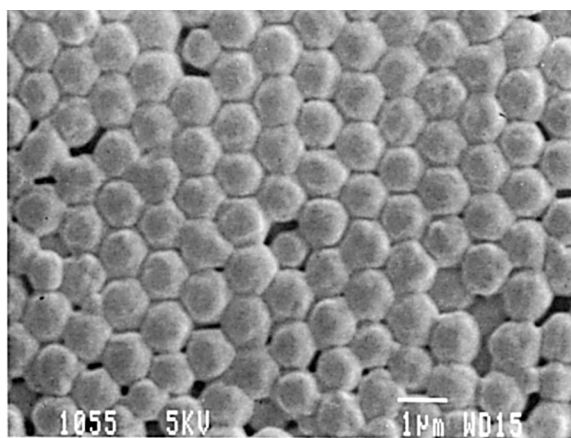
(e) Latex L10



(g) Latex L12



(f) Latex L11



(h) Latex L13

**Figure 1** (Continued from the previous page)

model for the range of potential conditions, i.e., the minimum radius of the circle of contact will occur when the polymer is dry during stage 2 and the particles undergo dry sintering. If, on the other hand, the polymer retains water during stage 2, fusion is a wet sintering process. Table V compares the experimental values of the radius of the circle of contact ( $a$ ) to the range of predicted values for a drying temperature of 22°C. The viscoelastic parameters were obtained at a frequency of 0.1 rad s<sup>-1</sup>.

Table V indicates that all the experimental values of " $a$ " (with the exception of latex L6) fall within the range predicted by the model. Some experimental data showed the particles to be fully fused. This parallels calculations where the value of " $a$ " exceeds the particle diameter, as for latexes L1–L4. The results of Table V are shown pictorially in Figure 2,

where the ordinate is expressed in terms of the particle radii and the dry polymer moduli. The expression given in the ordinate is a simplified version of eq. (2), where  $\eta^*$  is replaced by  $G^*/\omega$ . For the fully fused latexes (L1–L4), the radius is calculated on the following basis: Two spheres having radii  $R$  coalesce to form a single sphere having radius  $R'$ . The relationship between the radii is then  $R' = 1.26R$ .

The model predicts minimal fusion for highly rigid materials. Although the viscoelastic parameters reflect the character of the polymer, it would be expected that tight cross-linking (as in polymer L7) would prohibit polymer flow and result in hindered coalescence. In fact, the minimal film fusion for this material is in agreement with the model prediction, despite the physical restrictions due to the polymer morphology.

**Table V** Experimental and Predicted Values of the Radius of the Circle of Contact

Latex	Radius, $R$ (nm)	" $a$ " Experimental (nm)	" $a$ " Cap/ $\gamma_{p/a}$ <sup>a</sup> (nm)	" $a$ " Cap/ $\gamma_{p/w}$ <sup>b</sup> (nm)
L4	303.0	Fully fused	123.1	504.2
L3	340.0	Fully fused	203.8	845.7
L1	335.5	Fully fused	444.4	1754.4
L2	445.0	Fully fused	516.8	2029.9
L6	285.5	205.0	229.3	942.0
L10	350.0	—	171.1	716.2
L11	501.0	242.0	208.0	863.7
L12	450.0	231.0	106.4	456.6
L13	492.0	263.0	77.4	337.1

<sup>a</sup> Capillary force in tandem with dry sintering.<sup>b</sup> Capillary force in tandem with wet sintering.

There are some shortcomings to the model. The main failing of the model is its sensitivity to the magnitude of the viscoelastic parameters. An order of magnitude change in the frequency of data collection has a significant effect on the model prediction. Dynamic mechanical data were collected at a frequency of  $0.1 \text{ rad s}^{-1}$ , simply because the strain rates experienced by the polymer during film formation should be very low.

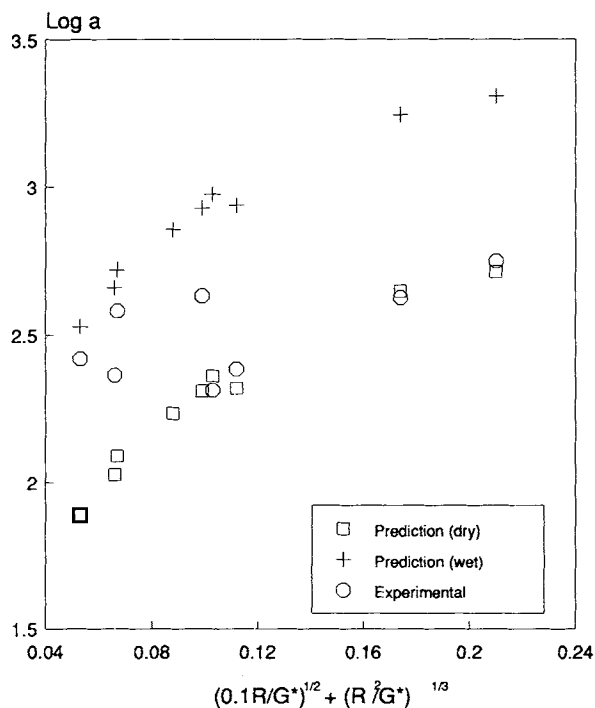


**Figure 2** Experimental and predicted values of the radius of the circle of contact as a function of the model parameters.

The polymer is assumed to behave in a viscoelastic manner. Dynamic mechanical analysis has shown this to be a valid assumption. In addition, the model is only valid for small strains, a condition that is obviously violated for very highly fused films. Also, the model is evaluated under the two extremes corresponding to the wet and dry polymers. In the wet case, the interfacial tension ( $\gamma_{p/w}$ ) between the polymer and water is considered to be one of the two driving forces for coalescence. However, the data of Ref. 11 indicate that the true value of  $\gamma_{p/w}$  cannot be determined because of water imbibition by the polymer, i.e., the exact nature of the surface is unknown. The parameter  $\gamma_{p/w}$  represents the interfacial energy between the dry hydrophilic copolymer surface and water and is the best value available. It is worth noting that recently Dobler et al.<sup>22</sup> synthesized model latexes with particular surface characteristics. These will presumably be utilized in further research into the film-formation phenomenon.

Other more detailed approaches to the problem are likely feasible. For instance, the particle system could be modeled in three dimensions: Drying kinetics would be related to the geometrical deformation of the spheres through the void fraction. The geometrical deformation would, in turn, be related to the physical character of the polymer. Evidently, this approach would be highly theoretical.

## CONCLUSIONS

The comprehensive model of film formation proposed in earlier work<sup>10</sup> was originally evaluated with respect to latex particle size. Experimental results for monodisperse latexes demonstrated that the de-



gree of film fusion is a function of particle radius, as predicted by the model. Small radius particles fuse more completely at room temperature. It was also concluded that minimum film temperature increases with increasing particle size. Several parameters were estimated in the preliminary assessment of the model. The effect of these variables was then considered in greater detail.

For the final analysis, the model was validated using an array of chemically similar polymers possessing widely different physical properties. All the measured parameters were included in the calculations. It was found that the model predictions for the radius of the contact region agreed with experimental observation. Also, the minimum film temperatures of the same polymers were determined. A dramatic rise in MFT was seen when the rigidity (or cross-linking) of the copolymer was increased. In other research,<sup>22</sup> lightly cross-linked copolymers were shown to form films with excellent mechanical properties. A high degree of coalescence is not required for good film performance.

This research was supported by the Natural Sciences and Engineering Research Council of Canada. The authors thank M. J. Devon for suggesting this research topic.

## REFERENCES

1. E. B. Bradford and J. W. Vanderhoff, *J. Macromol. Chem.*, **1**, 335 (1966).
2. S. S. Voyutskii, *J. Polym. Sci.*, **32**, 528 (1958).
3. W. E. Dillon, D. A. Matheson, and E. B. Bradford, *J. Colloid Sci.*, **6**, 108 (1951).
4. G. L. Brown, *J. Polym. Sci.*, **22**, 423 (1956).
5. G. Mason, *Br. Polym. J.*, **5**, 101 (1973).
6. D. P. Sheetz, *J. Appl. Polym. Sci.*, **9**, 3759 (1965).
7. J. Lamprecht, *Colloid Polym. Sci.*, **258**, 960 (1980).
8. K. Kendall and J. C. Padget, *Int. J. Adhes. Adhes.*, **2**, 149 (1982).
9. J. W. Vanderhoff, H. L. Tarkowski, M. C. Jenkins, and E. B. Bradford, *J. Macromol. Chem.*, **1**, 361 (1966).
10. S. T. Eckersley and A. Rudin, *J. Coat. Tech.*, **62**(780), 89 (1990).
11. S. T. Eckersley, A. Rudin, and R. O'Daiskey, *J. Coll. Int. Sci.*, **152**, 455 (1992).
12. S. T. Eckersley and A. Rudin, *Prog. Org. Coat.*, to appear.
13. S. G. Croll, *J. Coat. Tech.*, **59**(751), 81 (1987).
14. S. T. Eckersley and A. Rudin, *J. Appl. Polym. Sci.*, **48**, 1369 (1993).
15. D. P. Jensen and L. W. Morgan, *J. Appl. Polym. Sci.*, **42**, 2845 (1991).
16. M. J. Devon, T. Provder, and A. Rudin, *Measurement of Particle Size Distributions with a Disc Centrifuge. Data Analysis Considerations*, ACS Symposium Series 472, T. Provder, Ed., American Chemical Society, Washington, DC, 1991, p. 135.
17. T. F. Protzman and G. L. Brown, *J. Appl. Polym. Sci.*, **4**, 81 (1960).
18. ASTM D 2354-68, Standard Test Method for Minimum Film Formation Temperature (MFT) of Emulsion Vehicles, American Society for Testing Materials, Philadelphia, PA.
19. E. B. Bradford and J. W. Vanderhoff, *J. Macromol. Sci.-Phys.*, **B6**, 671 (1972).
20. N. Pramojaney, G. W. Poehlein, and J. W. Vanderhoff, in *Drying '80*, A. S. Mujumdar, Ed., Hemisphere, Washington, D.C., 1980, Vol. 2, pp. 93-100.
21. F. Dobler, T. Pith, Y. Holl, and M. Lambla, *J. Appl. Polym. Sci.*, **44**, 1075 (1992).
22. S. T. Eckersley, A. Rudin, and A. Plumtree, *J. Appl. Polym. Sci.*, **48**, 1689 (1993).

Received August 31, 1993

Accepted March 3, 1994